

Molecular Modeling, Synthesis, and Screening of New Bacterial Quorum-sensing Antagonists

KIM, CHEOLJIN¹, JAE EUN KIM¹, HYUNG-YEON PARK², ROBERT J. C. MCLEAN³,
CHAN KYUNG KIM², JONGHO JEON¹, SONG-SE YI¹, YOUNG GYU KIM¹, YOON-SIK LEE¹,
AND JEYONG YOON^{1*}

¹School of Chemical & Biological Engineering, Seoul National University, Seoul 151-742, Korea

²Department of Chemistry, College of Natural Science, Inha University, Incheon 402-751, Korea

³Department of Biology, Texas State University, 601 University Drive, San Marcos, TX 78666-4616, U.S.A.

Received: January 29, 2007

Accepted: March 9, 2007

Abstract A new series comprising 7 analogs of *N*-(sulfanyl ethanoyl)-L-HSL derivatives, 2 analogs of *N*-(fluoroalkanoyl)-L-HSL derivatives, *N*-(fluorosulfonyl)-L-HSL, and 2,2-dimethyl butanoyl HSL were synthesized using a solid-phase organic synthesis method. Each of the 11 synthesized compounds was analyzed using NMR and mass spectroscopies, and molecular modeling studies of the 11 ligands were performed using SYBYL packages. Thereafter, a bacterial test was designed to identify their quorum-sensing inhibition activity and antifouling efficacy. Most of the synthesized compounds were found to be effective as quorum-sensing antagonists, where antagonist screening revealed that 10 among the 11 synthesized ligands were able to antagonize the quorum sensing of *A. tumefaciens*.

Keywords: Quorum-sensing antagonists, binding energies, *N*-(sulfanyl ethanoyl)-L-HSLs, FlexX docking

By activating a signal transduction substance (known as an autoinducer or quorumone) with a low molecular mass, regulator protein, and sensor kinase, bacteria can sense the presence of other bacteria and thereby perform cell-cell communication to express specific genes. In this process, the concentration of the signal transduction substance is directly proportional to the number of bacteria, and the sensing of a critical level of a signal transduction substance is referred to as “quorum sensing (QS),” a mechanism wherein the cells begin to reveal themselves [6, 7, 22].

Since QS is closely related to virulence and biofilm formation, its disturbance by anti-QS agents can provide clues for the development of novel antibiotics. Gram-negative bacteria mainly produce a series of *N*-acyl-

homoserine lactone (AHL) compounds as signal molecules [12, 14, 20].

Thus, investigating autoinducer antagonists has attracted a lot of attention [3, 4, 17, 24, 26], and it has been reported that *N*-(2,2-difluorodecanoyl)-L-HSL, developed by Kline *et al.* [14], has an excellent ability to inhibit biofilm formation [15]. Furthermore, based on a report that 2-vinyl-2,3-dihydro-1,4-dithiine cyclic sulfur compounds, extracted from garlic, can inhibit QS, Persson *et al.* [20] used a solution-phase synthesis method to synthesize a molecule containing sulfur bound to the main chain of AHL. They also reported that the synthesized compound was effective as a QS antagonist [21].

Accordingly, this article focuses on a series of inhibitors that could act as antagonists against *N*-3-oxoalkanoyl HSL, a quorum-sensing signal of *Pseudomonas aeruginosa* and *Agrobacterium tumefaciens*. These species of Gram-negative bacteria cause various diseases and form a biofilm using signal transduction molecules, making it very important to develop antagonists against these autoinducers.

After studying the structure of *N*-3-oxoalkanoyl HSL (Fig. 1), a new inhibitor was synthesized by replacing the ketone moiety at the 3rd carbon of the analogs with sulfur [2].

Although this idea originated from the study of Persson *et al.* [20], the present study used a solid-phase synthesis method, and instead of an alkyl group, groups with different

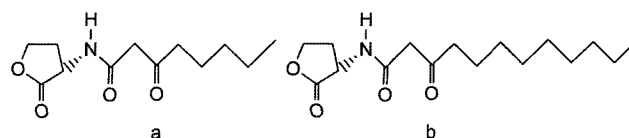


Fig. 1. *N*-3-oxooctanoyl-L-HSL (QS signal molecule of *Agrobacterium tumefaciens*, a) and *N*-3-oxododecanoyl-L-HSL (QS signal molecule of *Pseudomonas aeruginosa*, b).

*Corresponding author

Phone: 82-2-880-8927; Fax: 82-2-876-8911;
E-mail: jeyong@snu.ac.kr

molecular structures, such as hetero ring compounds, were bonded to the tail portion of AHL. The yield of a solid-phase organic synthesis (SPOS) method is higher than that of a solution-phase organic synthesis method, plus the former facilitates combinatorial organic synthesis. In particular, since molecules with an L-type enantiomer at the asymmetrical carbon atom show a higher degree of antagonism, it is more effective to synthesize the required 3-dimensional structure [1], which is one advantage of an SPOS method. In addition, using the *N*-(2,2-difluorodecanoyl)-L-HSL developed by Kline *et al.*, new analogs were synthesized by replacing the fluoride with a methyl group or the hydrogen with a fluoride using the SPOS method.

MATERIALS AND METHODS

Chemicals

An aminomethyl polystyrene resin was purchased from Beadtech Inc., Korea, and the other chemicals were purchased from Sigma-Aldrich. All the solvents were purified and dried before use.

Procedures for Solid-phase Synthesis

As shown in Fig. 2, a solid-phase synthetic method was applied to synthesize 11 new quorum-sensing antagonists, in the form of *N*-(alkylsulfanylethanoyl)-L-HSL derivatives, *N*-(fluoroalkanoyl)-L-HSL derivatives, *N*-(fluorosulfonyl)-L-HSL, or 2,2-dimethyl butanoyl-L-HSL [16]. Ten g (22 mmol) of an aminomethyl polystyrene resin (AM PS, 200–400 mesh, 2.2 mmol/g, Beadtech Inc., South Korea) was swollen in 100 ml of *N*-methyl-2-pyrrolidone (NMP) in a 3-neck flask (250 ml). To introduce a methionine residue onto the resin, *N*-Fmoc-methionine (14.86 g,

40 mmol), 1-hydroxybenzotriazole (HOBT, 5.33 g, 40 mmol), diisopropyl ethylamine (DIEA, 5.17 g, 40 mmol), and benzotriazol-1-yl-oxy-tris(dimethylamino)phosphonium hexafluorophosphate (BOP, 17.69 g, 40 mmol), acting as coupling agents, were added to the flask. The solution was then stirred at room temperature for 24 h, and the completion of the reaction determined using a Ninhydrin color test. After filtering the *N*-Fmoc methionine-coupled resin, the resin was washed two or three times with NMP, methylene chloride (MC), and methanol, followed by drying *in vacuo* (mass increase: 8.17 g; yield: 99.82%). The resin was confirmed to contain an amide bond as a result of the coupling reaction based on the FT-IR spectrum, which showed amide peaks at 1,718 and 1,670 cm^{-1} . To remove the Fmoc group from the *N*-Fmoc methionine-mediated resin, the resin (11 g) was then treated twice with piperidine/dimethylformamide (DMF) (20%, v/v) at room temperature for 1 h each time. Thereafter, the resin was filtered, washed two or three times with DMF, MC, and methanol, and dried *in vacuo* to measure its final mass (7.13 g). A Ninhydrin test indicated that the solution contained an amine group, although the amide band disappeared from the FT-IR spectrum (1,718 cm^{-1}). The Fmoc-removed resin (500 mg) was then swollen in NMP (15 ml) in each of the eleven filtered reactors (Libra tube RT-20M, Beadtech Inc., South Korea). The resin was reacted with the *N*-(alkylsulfanylethanoyl)-L-HSL derivatives, *N*-(fluoroalkanoyl)-L-HSL derivatives, *N*-(fluorosulfonyl)-L-HSL, or 2,2-dimethyl butanoyl-L-HSL (2.8 mmol) in the presence of HOBT (378.28 mg, 2.8 mmol), BOP (1,238.44 mg, 2.8 mmol), and DIEA (361.9 mg, 2.8 mmol). The reaction was carried out at room temperature for 24 h, and then the reaction mixture was filtered and washed with NMP, MC, and methanol, followed by drying *in vacuo*. The reaction yield was investigated based on the mass increase, which ranged from 90% to 94%. To prepare a series of homoserine lactones, the resin was treated with BrCN (860 mg, 8 mmol) and trifluoroacetic acid (TFA, 5%) in chloroform/water (10 ml/5 ml) in each of the 11 filtered reactors. The homoserine lactone derivative products were then cleaved from the beads twice for 12 h using a chemical cleavage method. Thereafter, the resin was filtered and washed two or three times with chloroform, and then the cleavage and washing solution were collected in a round-bottom flask (100 ml) and the chloroform layer separated. The collected solution was extracted several times with CHCl_3 and brine, and then the final chloroform solution was evaporated. As a result, homoserine lactone products with yields ranging from 68% to 79% were obtained from the AM PS resin [5a (79%), 5b (78%), 5c (68%), 5d (79%), 5e (71%), 5f (78%), 5g (70%), 5h (79%), 5i (73%), 5j (69%), 5k (77%)]. **2-Oxo-2-(2-oxotetrahydrofuran-3-ylamino)ethyl benzodithioate (5d)**: $^1\text{H NMR}$ (CDCl_3 , 400 MHz) δ =8.03 (s, 1H, NH), 7.45–7.41 (m, 3H, Ar-H), 7.3 (d, J=5.4 Hz,

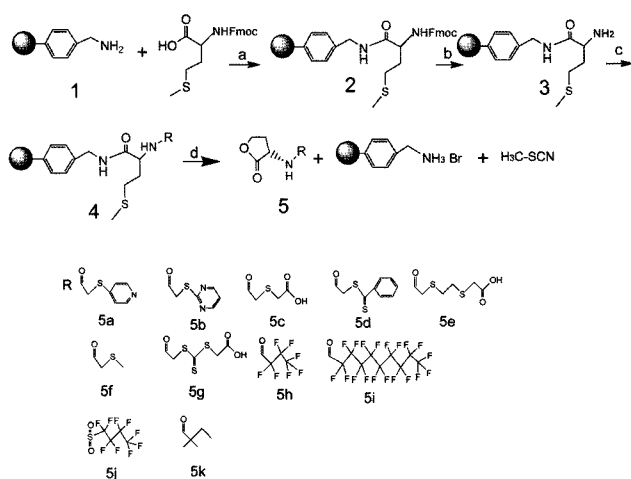


Fig. 2. Synthesis of new analogs (a) DIEA, HOBT, BOP, NMP, 25°C; (b) 20% piperidine/DMF, 25°C; (c) DIEA, HOBT, BOP, carboxylic acid or sulfonyl chloride, NMP, 25°C; (d) BrCN, CF_3COOH , $\text{CHCl}_3/\text{H}_2\text{O}$, 25°C.

2H, Ar-H), 4.52–4.21 (m, 3H, CH-Lac), 3.78 (s, 2 H, CH₂), 2.46–2.39 (m, 1 H, CH-Lac), 2.22–2.17 (m, 1 H, CH-Lac); HRMS (CI) calcd for C₁₃H₁₃NO₃S₂ (M⁺+1) 295.3832, found 295.3831.

Bioassay

Autoinducer Bioassay. In the experiment designed to identify the quorum-sensing antagonist, *Agrobacterium tumefaciens* A136 (pTiA136, pCF218, pCF372), which had been mutated to produce β-galactosidase by expressing the *lac* gene when exposed to HSL, and *Agrobacterium tumefaciens* KYC6, which had been mutated to overproduce AHL, were used as the indicating microorganisms, along with 5-bromo-4-chloro-3-indolyl-β-D-galactopyranoside (X-gal), which gives off a green or blue color when degraded by the β-galactosidase produced during the same process as an indicating material [8, 9, 18, 19]. For the experiment, the KYC6 type-culture strain was cultured overnight in an LB broth at 30°C, and then 10 μl of the KYC6 strain and 100 μl of the sample solution were inoculated into 5 ml of an LB broth and cultured for 24 h at 30°C. The A136 strain was also cultured overnight at 30°C in an LB broth containing 50 μg/ml of spectinomycin and 4.5 μg/ml of tetracycline. Instead of the sample solution, distilled water was used for the control experiment. Sixteen μl of an X-gal/DMF solution and 50 μl of distilled water were spread on an LB agar. The A136 strain was then streaked onto the middle of the LB agar plate using a platinum loop. Thereafter, the KYC6 strains cultured with the sample solution were streaked 1–2 cm away from the A136 line, and the LB agar plates incubated for two days until a green or blue color was found in the control sample at 30°C. The synthesized antagonist was then evaluated in terms of how competitively it inhibited the activities of the AHL (acylhomoserine lactone) automatically produced by *Agrobacterium tumefaciens* KYC6 (Table 1).

Library Screening for Antagonists. *Agrobacterium tumefaciens* A136 (pTiA136, pCF218, and pCF372) was selected as the reporter strain, and cultured in Luria-Bertani (LB) media with 50 μg/ml spectinomycin and 4.5 μg/ml tetracycline at 30°C [19]. For the antagonist assay, an overnight culture was diluted to achieve an optical density of 0.3 at 600 nm (OD₆₀₀). The autoinducer (AI) and antagonist samples were prepared as chloroform solutions, and then 4 μl of the autoinducer (3-oxo-C₈-HSL;

final concentration, 0.5 μM) and 40 μl of the 11 antagonist samples (final concentration, 5 μM) were added to the test tubes. After the chloroform was vaporized, 4,000 μl of the diluted strain culture was added and incubated for 3 h at 30°C. The LacZ bioassay was conducted using a Tropix-plus kit (T1011, Applied Biosystems, U.S.A.), the luminescence measured using a luminescence meter (Thermo electron Co., U.S.A.), and the OD₆₀₀ values measured using a UV spectrophotometer (HP8452A, H.P., U.S.A.). The antagonist activities of the compounds were expressed as the relative luminescence/OD₆₀₀ values.

Biofilm Formation Assay. To evaluate the biofilm formation-inhibiting activity of the antagonist samples, the biofilm of *Pseudomonas aeruginosa* PA01-GFP (green fluorescent protein), well defined for biofilm formation, was grown using a CDC (Center for Disease Control) reactor [25, 28]. The inoculum PA01-GFP stock was cultured in 1/10 Tryptic Soy Broth media for 20–24 h at 37°C, and then 1 ml of the prepared stock was inoculated into a sterilized reactor with 100 ml of 1/100-strength TSB and 20 μg/ml of each antagonist sample. The initial PA01 population of the batch media was about 10⁵ CFU/ml. The reactor was operated in the batch mode for 24 h at 100 rpm and room temperature. Thereafter, the reactor was connected via a nutrient feed line to a carboy containing 1/300 strength TSB with 1 μg/ml of each sample and operated in a continuous flow mode at a 10 ml/min flow rate for 24 h. Distilled water was used instead of the antagonist samples for the control experiment. After 24 h, coupons were collected in 10 ml of a phosphate-buffered solution and the biofilms on the coupon disaggregated by 1 min of sonication. One ml of each suspended solution was used for colony counting, and the CFU values were determined after 24 h of incubation at 37°C. The coupons for microscopic analysis were imaged using an epifluorescence microscope (Nikon H550L, Japan).

Molecular Modeling Study

To examine the binding energy of the 11 ligands, molecular modeling studies were performed using SYBYL packages [27]. In a previous X-ray crystallographic study, the quorum-sensing transcription factor was reported as complexed with an autoinducer and DNA (PDB code= 1L3L) [29]. Moreover, a complex crystal structure allows the binding mode at an active site to be easily identified. Therefore, molecular modeling of the newly designed

Table 1. List of strains used.

Strain	Description	Purpose
<i>A. tumefaciens</i> A136 ^a	<i>traI-lacZ</i> fusion(pCF218)(pCF372)	AHL biosensor
<i>A. tumefaciens</i> KYC6 ^a	3-oxo-C ₈ HSL overproducer	Positive control for AHL assay
<i>P. aeruginosa</i> PA01	Biofilm-forming indicator	Biofilm formation assay

^aSource or reference; Fuqua and Winans [9].

ligands was performed to examine the structural features of their interactions at an active site. The FlexX dockings of the ligands were modeled using the Run-Multiple ligand option of FlexX [13]. Optimal conformational poses were selected from among several possibilities based on the values obtained for the root-mean-square (RMS) deviation from the reference structure.

RESULTS AND DISCUSSION

First, the specific-binding interaction between a receptor and a reference ligand (autoinducer) was investigated in three-dimensional space using the FlexX package [13, 27, 29]. The autoinducer (AI) ligand in the crystal structure (stick representation) and best-docked structure (yellow ball-and-stick representation) are shown in Fig. 3A. The RMS deviation between the two structures was 0.62 Å, suggesting that the FlexX docking result was reliable. The AI ligand has several functional groups that can interact with a receptor, such as a lactone group, polar group (an amide bond and nearby carbonyl group), and hydrocarbon chain. In the docking structure, the ligand forms two hydrogen bonds (H bonds) with active-site residues (carbonyl oxygen of the lactone moiety with the ϵ nitrogen of Trp57, and N-H of the polar moiety with the carbonyl oxygen of Asp70). Two carbonyls from the polar group are capable of polar interactions with the side chains of Tyr53 and Thr129. Since several aromatic and hydrophobic residues form the binding pocket, the active-site region is

believed to be more hydrophobic than the reference ligand (for example, $\log P(\text{AI}) = -0.478$ and $\log P(\text{Phe}) = -1.605$). The hydrocarbon chain is surrounded by several residues, including Tyr53, Leu40, Tyr61, and Phe62, which can be stabilized by hydrophobic interactions.

Fig. 3B depicts the active-site region as a MOLCAD surface [11] for visual characterization of the binding property: the ligand was positioned on top of the surface. This figure reveals that the binding region for the lactone moiety is narrow, yet becomes wider for the binding of the polar and hydrocarbon moieties. Note, there are a few polar regions near the terminal carbon chain that can form additional H bonds or participate in polar interactions. Since a lactone moiety is invariably present in all the autoinducers of the LuxR family of cell-density-responsive transcriptional regulators [8, 9], the new ligands were designed by altering the polar and carbon chain moieties.

In this study, the molecular dockings between a receptor and the 11 designed molecules were performed using FlexX to identify differences in the biological activities of the ligands. The structures of all the designed ligands were sketched and minimized using a Tripos force field [5] until the RMS gradient was less than 0.05. The 11 ligands are shown in Scheme 2 and classified into three groups. In group I, the hydrophobicity was decreased or increased with changes in the length of the polar group moiety or by the addition of a lipophilic group (5a, 5b, 5d, 5f, and 5k). In group II, a carboxyl group was added at the terminal group to form H bonds with the binding pocket (5c, 5e, and 5g). In group III, hydrogen atoms were substituted

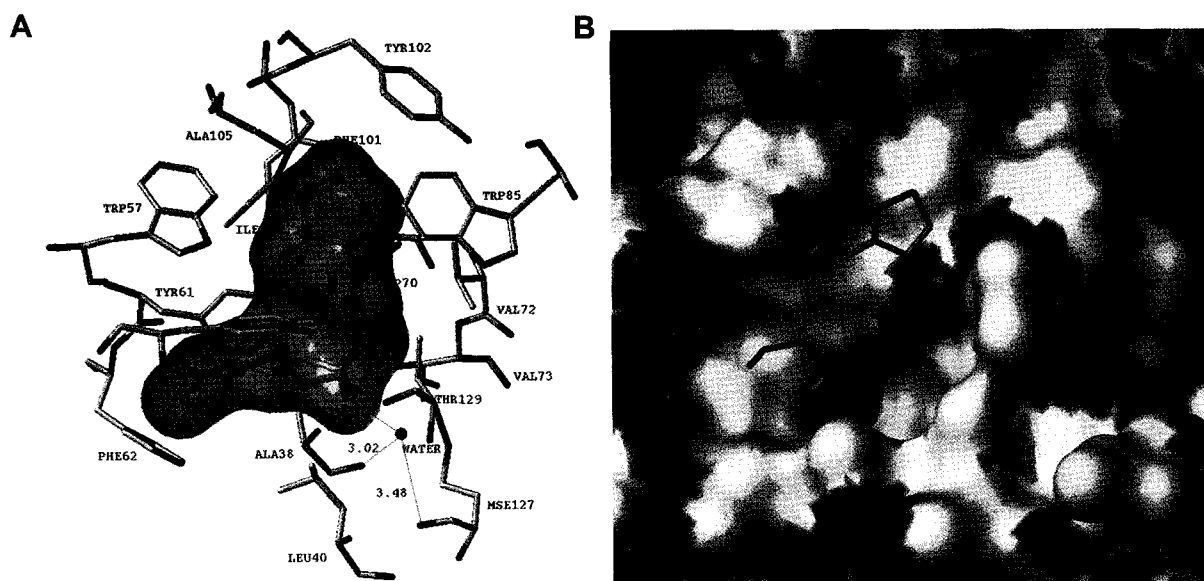


Fig. 3. A. View of the AI ligand in the binding cavity of the protein. The AI in the crystal structure and protein residues are represented as sticks, whereas the AI in its FlexX best-docked pose is shown as a ball-and-stick representation. The oxygen, nitrogen, and carbon atoms are colored red, blue, and grey, respectively. The cavity is depicted as a transparent surface. B. MOLCAD surface of the ligand-binding pocket. The ligand is positioned on top of the surface. The oxygen, nitrogen, carbon, and sulfur are colored red, blue, white, and yellow, respectively.

Table 2. Binding energies of best-docked structures.

Ligand	Binding energy (kcal/mol)
AI	-12.78
5a	-15.33
5b	-10.53
5c	-14.09
5d	-20.17
5e	-14.71
5f	-14.62
5g	-12.91
5h	-14.34
5i	-5.93
5j	-11.05
5k	-15.40

with fluorine atoms to identify any possible H bonds or polar interactions with the binding pocket (5h, 5i, and 5j). The ligands were docked on a receptor using the same strategy as described above. The FlexX docking scores (or binding energies in kcal/mol) of the AI and 11 ligands are summarized in Table 2. Except for three ligands (5b, 5i, and 5j), the binding scores for the designed ligands were better than those for the reference ligand, suggesting that most of the designed ligands had a better inhibition activity than the reference ligand.

Among the ligands belonging to group I, 5f and 5k had no polar carbonyl or hydrocarbon groups, and these ligands had binding energies lower than that of the AI. When an aromatic or heteroaromatic group was present at the terminal position (5a, 5b, and 5d), 5d exhibited the best binding score (-20.17 kcal/mol), whereas 5b exhibited the worst score (-10.53 kcal/mol). The docking poses of these ligands are depicted in Fig. 4A. The lactone was present at almost the same position in the reference ligand as in all the designed ligands. The only difference that could explain

the different bioactivities was the three-dimensional orientation of the polar and terminal groups. In 5b, the pyrimidine ring appeared to form an H bond with Tyr61, yet close contact between the phenyl and pyrimidine rings caused severe bumping and inhibited such binding. 5a had a better pose at the active site, yet this pose was not sufficient for maximal hydrophobic interaction with the active-site residues. The best pose was observed in the case of 5d, which had maximal hydrophobic interaction without bumping with the active-site residues.

From the analysis of the binding pocket shown in Fig. 3B, the group II ligands could form H bonds with the polar region of the binding pocket, as shown in Fig. 4B, which depicts the best poses for the group II ligands. As shown in Fig. 4B, 5c, 5e, and 5g could form favorable H bonds with Tyr61, Gln58, and Thr51, respectively. Furthermore, hydrophobic interactions with binding-site residues are another important stabilizing factor. Although such interactions were not possible for 5c owing to its shorter chain length, the ligand with the longest chain length, *i.e.*, 5e, had perfect positioning for hydrophobic interactions, thereby exhibiting the best activity and best binding energy among the group II ligands.

To examine the possible H bonds or polar interactions with the binding pocket, compounds with perfluorinated carbons chain were synthesized and tested (group III). Contrary to the experimental results (*vide infra*) shown in Fig. 4C, 5i and 5j showed worse binding energies than the AI. The FlexX docking pose for each ligand is shown in Fig. 4C. Whereas 5i could form an H bond with Thr51, 5j could not form any H bond with the binding-pocket residues. Moreover, the perfluorinated groups exhibited strong repulsive interactions with the hydrophobic binding pocket, as the F atom had the highest electronegativity. No such repulsive interaction was possible in the case of 5h owing to its shorter carbon-chain length. The discrepancy

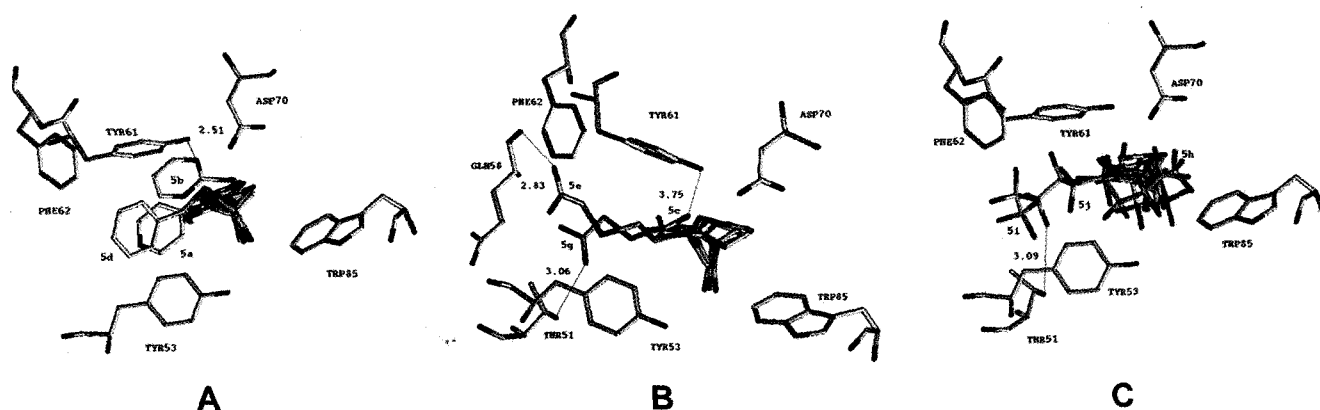


Fig. 4. A. Best poses of 5a, 5b, and 5d at the binding site. Hydrogen atoms have been removed for clarity (group I). B. Best poses of 5c, 5e, and 5g at the binding site. Hydrogen atoms have been removed for clarity (group II). C. Best poses of 5h, 5i, and 5j (hidden) at the binding site. Hydrogen atoms have been removed for clarity (group III).

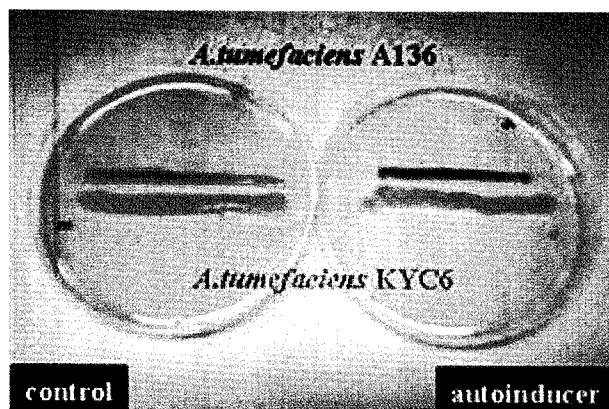


Fig. 5. Bioassay for autoinducer detection. The color of the synthesized autoinducer is considerably darker than that of the reference.

between the experimental and theoretical results for 5i and 5j can be explained if protein flexibility is considered during the docking process.

The molecular modeling was performed using SYBYL packages, and the binding pose of the reference ligand used to identify important H bonds and hydrophobic interactions. Additionally, the bioactivities of the 11 designed ligands were explained based on their FlexX binding energies and best docking poses. The ligands with the following properties exhibited higher binding energies and bioactivities: hydrophobic interaction (5d), additional H bonds and hydrophobic interactions (5e and 5g), and no appreciable repulsive interactions (5f, 5h, and 5k) with the binding pocket. The binding energies of the perfluorinated ligands (5i and 5j) were not considered owing to the strong repulsive interactions of these ligands with the binding-site residues.

The QS inhibition and antifouling tests used a solution concentration of 1 $\mu\text{mol/l}$, and Fig. 5 shows the experimental results for the activities of the autoinducer *N*-3-oxobutanoyl-L-HSL. In the experiment with the autoinducer, the color of the sample plate was clearly darker than that of the reference. When *A. tumefaciens* KYC6, which had been mutated to overproduce AHL, was cultured at a distance of 1–2 cm from the reporter strain *A. tumefaciens* A136 (pCF218) (pCF372), it produced a green color in the bioassay medium due to active expression of the *lacZ* reporter gene. Furthermore, when *A. tumefaciens* KYC6 was cultured with a solution containing the synthesized autoinducer, it produced a dark blue color in the bioassay medium due to the accelerated expression of the *lacZ* reporter gene, which indicates that *N*-3-oxobutanoyl-L-HSL was able to promote the QS reporter system.

The experimental activities for the synthesized antagonists are shown in Fig. 6, where all showed a smaller degree of color change in the sample plate than in the reference,

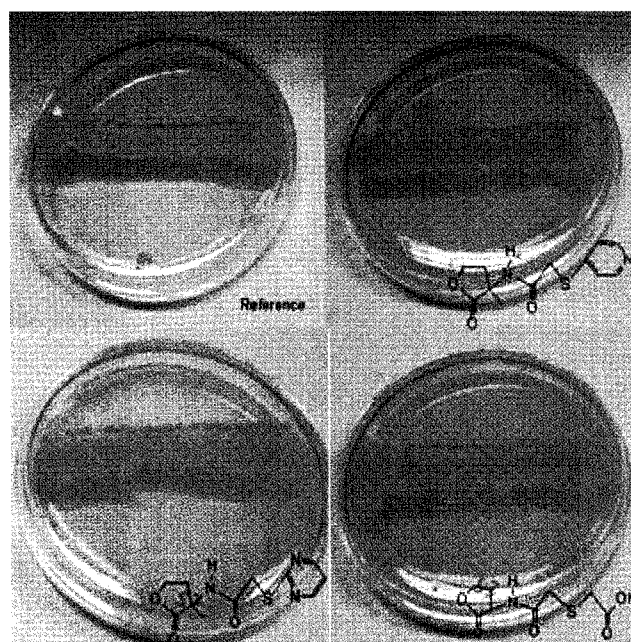


Fig. 6. Bioassay for new antagonists. The antagonists show a smaller color change than the reference (5a, 5b, 5c).

thereby verifying their antagonism. When *A. tumefaciens* KYC6 was cultured with a solution containing a synthesized antagonist, it produced a light blue color in the bioassay medium due to reduced expression of the *lacZ* reporter gene [10]. One interpretation is that the new antagonists competed with the autoinducers for a very specific interaction with the traR protein [23]. Thus, the inhibitory activity of the modified HSL antagonists most likely resulted from their interaction with several amino acids of the traR protein in the region containing the *N*-acyl-L-HSL binding site or in the dimerization domain. It is already known that traR, the receptor protein or transcriptional regulator from *A. tumefaciens*, only activates gene transcription after dimerization [10, 23], which implies that traR requires the binding of *N*-acyl-L-HSL prior to the transcriptional activation of the target promoters. However, the new antagonists prevented *N*-acyl-L-HSL from activating the gene transcription, thereby explaining the smaller degree of color change in the sample plate than in the reference. Consequently, it was proven that the 10 newly synthesized *N*-(alkylsulfanylethanoyl)-L-HSL, *N*-(fluoroalkanoyl)-L-HSL, *N*-(fluorosulfonyl)-L-HSL, or 2,2-dimethyl butanoyl-L-HSL QS antagonists exhibited antagonistic activity.

The 11 new ligands were also tested for their antagonist activity using the reporter strain *A. tumefaciens* A136 (pTiA136, pCF218, and pCF372) to identify compounds that could compete against the AI and repress *traI::lacZ*-operon expression. The *A. tumefaciens* was grown for 3 h

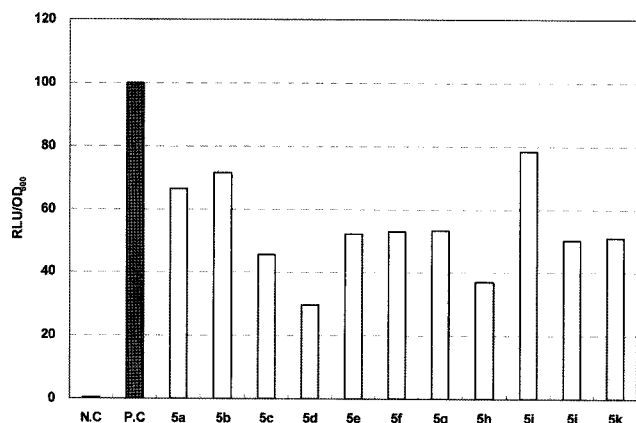


Fig. 7. Quorum-sensing antagonist assays *A. tumefaciens* was grown for 3 h in the presence of 0.5 μ M AI (positive control, P.C.) or 0.5 μ M AI with 5 μ M of the antagonists (5a–5k).

in the presence of either 0.5 μ M of the AI or 0.5 μ M of the AI and 5 μ M of the antagonist samples. The luminescence intensity was divided by the OD₆₀₀ value of the cell culture, plus the control was set at 100%, and all the other values determined relative to that of the control. As shown in Fig. 7, the luminescence assays performed on the 11 new quorum-sensing antagonists revealed that the luminescence intensity decreased by 22% to 72%, implying that the solutions containing the synthesized antagonists suppressed the *traI::lacZ*-operon gene expression. All the synthesized analogs, except for **5i**, were potent QS antagonists. Analog

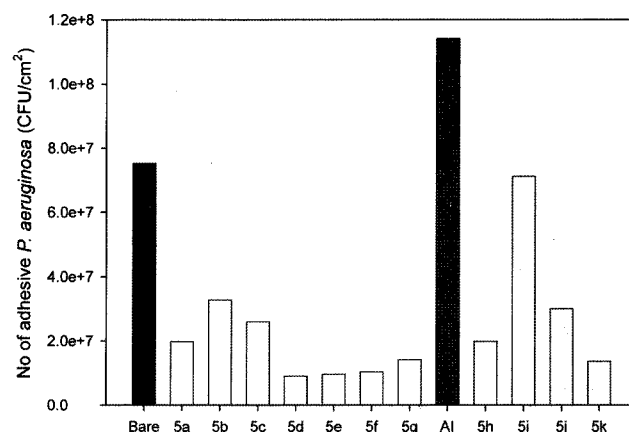


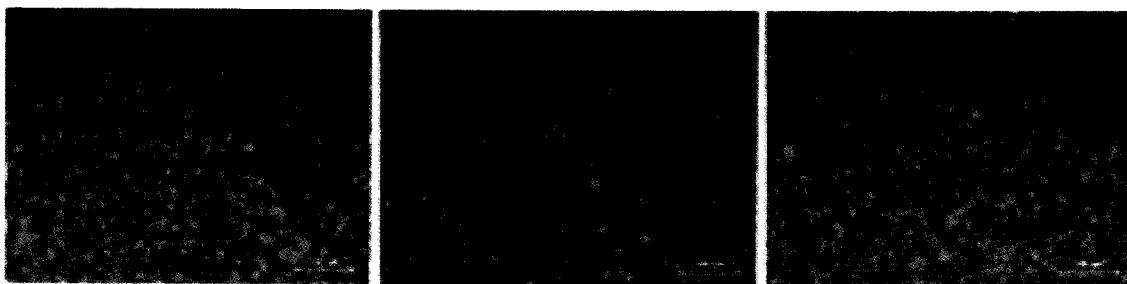
Fig. 8. Number of adhesive *P. aeruginosa* on the surface after 4 h.

5d produced the best result and also had the best FlexX docking score.

As shown in Fig. 8, the antifouling tests conducted on all 11 of the new QS antagonists showed that the extent of *P. aeruginosa* adhesion decreased by 10–80%, indicating that the 10 analogs among the 11 newly synthesized compounds possessing an *N*-(alkylsulfanylethanoyl)-L-HSL, *N*-(fluoroalkanyoyl)-L-HSL, *N*-(fluorosulfonyl)-L-HSL, or 2,2-dimethyl butanoyl-L-HSL moiety are potential compounds for disrupting the QS system of *P. aeruginosa*.

Microscopic images depicting the results of the antibiofouling test are shown in Fig. 9. The biofilms were

Control



Antagonist



Fig. 9. Micrographs of *P. aeruginosa* biofilms grown on glass slides after 48 h in negative control with distilled water (upper) or synthetic antagonist (**5d**, bottom).

grown for 48 h in the presence of an antagonist or distilled water, and the resulting micrographs show that the newly synthesized antagonists prohibited the formation of the *P. aeruginosa* biofilm. As shown in Fig. 9, *P. aeruginosa* grown in a reactor in the presence of the synthetic antagonists showed planktonic growth. Furthermore, the number of cells attached to the surface was small. In contrast, *P. aeruginosa* grown in a reactor in the presence of distilled water adhered and started forming a biofilm. The cells from samples containing an antagonist generated less biofilm, as observed in the micrographs. Therefore, the series of 10 QS inhibitors among the 11 synthesized compounds exhibited an antifouling efficacy. The bioassay results for the new compounds were also similar to the results of the molecular modeling study.

In conclusion, new biologically active antagonists were discovered and 11 new *N*-(alkylsulfanylethanoyl)-L-HSL, *N*-(fluoroalkanoyl)-L-HSL, *N*-(fluorosulfonyl)-L-HSL, or 2,2-dimethyl butanoyl-L-HSL QS antagonists were synthesized with considerably high yields due to the nature of the synthesis method used. The 10 new analogs of *N*-acyl HSL or *N*-sulfonylhomoserine lactone derivatives were also shown to act as antagonists against *N*-3-oxoalkanoyl HSL, one of the autoinducers of *Agrobacterium tumefaciens* and *Pseudomonas aeruginosa*. Therefore, the use of molecular modeling to seek new QS antagonists was shown to be very effective, and the present results suggest that the 10 new analogs among the 11 synthesized compounds could be potent QS antagonists and antifouling agents.

Acknowledgments

The authors are grateful to Prof. Lee Kyu-Ho at Hankuk University of Foreign Studies for helping with the bioassay. This research was partially supported by the Brain Korea 21 Program (Korean Ministry of Education). The authors wish to acknowledge the financial support by Seoul R & D Program (10538), through Institute of Bioengineering, Seoul National University, Seoul, Korea.

REFERENCES

- Arya, P. and M. G. Baek. 2001. Natural product-like, chiral derivatives by solid phase synthesis. *Curr. Opin. Chem. Biol.* **5**: 292–301.
- Bassler, B. L., M. Wright, and M. R. Silverman. 1994. Multiple signaling systems controlling expression of luminescence in *Vibrio harveyi*: Sequence and function of genes encoding a second sensory pathway. *Mol. Microbiol.* **13**: 273–286.
- Baveja, J. K., G. Li, R. E. Nordon, E. B. H. Hume, N. Kumar, M. D. P. Willcox, and L. A. Poole-Warren. 2004. Biological performance of a novel synthetic furanone-based antimicrobial. *Biomaterials* **25**: 5013–5021.
- Castang, S., B. Chantegrel, C. Deshayes, R. Dolmazon, P. Gouet, R. Haser, S. Reverchon, W. Nasser, N. Hugouvieux-Cotte-Pattat, and A. Doutheau. 2004. *N*-Sulfonyl homoserine lactones as antagonists of bacterial quorum sensing. *Bioorg. Med. Chem. Lett.* **14**: 5145–5149.
- Clark, M., R. D. Cramer III, and N. Van Opdenbosch. 1989. Validation of the General Purpose Tripos 5.2 Force Field. *J. Comp. Chem.* **10**: 982–1012.
- Daniels, R., J. Vanderleyden, and J. Michiels. 2004. Quorum sensing and swarming migration in bacteria. *FEMS Microbiol. Rev.* **28**: 261–289.
- Defoirdt, T., N. Boon, P. Bossier, and W. Verstraete. 2004. Disruption of bacterial quorum sensing: An unexplored strategy to fight infections in aquaculture. *Aquaculture* **240**: 69–88.
- Fuqua, C., M. Burbea, and S. C. Winans. 1995. Activity of the *Agrobacterium* Ti plasmid conjugal transfer regulator TraR is inhibited by the product of the *traM* gene. *J. Bacteriol.* **177**: 1367–1373.
- Fuqua, C. and S. C. Winans. 1996. Conserved cis-acting promoter elements are required for density-dependent transcription of *Agrobacterium tumefaciens* conjugal transfer genes. *J. Bacteriol.* **178**: 435–440.
- Fuqua, C. and E. P. Greenberg. 1998. Self perception in bacteria. *Curr. Opin. Microbiol.* **1**: 183–189.
- Ghose, A. K. and G. M. Crippen. 1986. Atomic physicochemical parameters for three-dimensional structure-directed quantitative structure-activity relationships I. Partition coefficients as a measure of hydrophobicity. *J. Comp. Chem.* **7**: 565–577.
- He, X. and C. Fuqua. 2006. Rhizosphere communication: Quorum sensing by the rhizobia. *J. Microbiol. Biotechnol.* **16**: 1661–1677.
- Jacek, S., B. Markus, S. Isabel, D. Hans-Martin, and S. Martin. 2001. Synthesis, molecular modeling, and structure-activity relationship of benzophenone-based CAAX-peptidomimetic farnesyltransferase inhibitors. *J. Med. Chem.* **44**: 2886–2899.
- Jang, A., M. Bum, S. Kim, Y. Ahn, I. S. Kim, and P. L. Bishop. 2005. Assessment of characteristics of biofilm formed on autotrophic denitrification. *J. Microbiol. Biotechnol.* **15**: 455–460.
- Kline, T., J. Bowman, B. H. Iglewski, T. de Kievit, Y. Kakai, and L. Passador. 1999. Novel synthetic analogs of the *Pseudomonas* autoinducer. *Bioorg. Med. Chem. Lett.* **9**: 3447–3452.
- Ko, D. H., D. J. Kim, C. S. Lyu, I. K. Min, and H. S. Moon. 1998. New cleavage approaches to combinatorial synthesis of homoserine lactones. *Tetrahedron Lett.* **39**: 297–300.
- Manefield, M., T. B. Rasmussen, M. Henzter, J. B. Andersen, P. Steinberg, S. Kjelleberg, and M. Givskov. 2002. Halogenated furanones inhibit quorum sensing through accelerated LuxR turnover. *Microbiology* **148**: 1119–1127.
- McLean, R. J. C., M. Whiteley, D. J. Stickler, and W. C. Fuqua. 1997. Evidence of autoinducer activity in naturally occurring biofilms. *FEMS Microbiol. Lett.* **154**: 259–263.
- McLean, R. J. C., L. S. Pierson, and C. Fuqua. 2004. A simple screening protocol for the identification of quorum

- signal antagonists and antibiotics. *J. Microbiol. Meth.* **58**: 351–360.
20. Na, B. K., B. I. Sang, D. W. Park, and D. H. Park. 2005. Influence of electric potential on structure and function of biofilm in wastewater treatment reactor: Bacterial oxidation of organic carbons coupled to bacterial denitrification. *J. Microbiol. Biotechnol.* **15**: 1221–1228.
 21. Persson, T., T. H. Hansen, T. B. M. E. Rasmussen, M. Givskov, and J. Nielsen. 2005. Rational design and synthesis of new quorum-sensing inhibitors derived from acylated homoserine lactones and natural products from garlic. *J. Org. Biomol. Chem.* **3**: 253–262.
 22. Rasmussen, T. B. and M. Givskov. 2006. Quorum-sensing inhibitors as anti-pathogenic drugs. *Int. J. Med. Microbiol.* **296**: 149–161.
 23. Reverchon, S., B. Chantegrel, C. Deshayes, A. Doutheau, and N. Cotte-Pattat. 2002. New synthetic analogues of *N*-acyl homoserine lactones as agonists or antagonists of transcriptional regulators involved in bacterial quorum sensing. *Bioorg. Med. Chem. Lett.* **12**: 1153–1157.
 24. Smith, K. M., Y. Bu, and H. Suga. 2003. Library screening for synthetic agonists and antagonists of a *Pseudomonas aeruginosa* autoinducer. *Chem. Biol.* **10**: 563–571.
 25. Speranza, G., G. Gottardi, C. Pederzoli, L. Lunelli, R. Canteri, L. Pasquardini, E. Carli, A. Lui, D. Maniglio, M. Brugnara, and M. Anderle. 2004. Role of chemical interactions in bacterial adhesion to polymer surfaces. *Biomaterials* **25**: 2029–2037.
 26. Stoodley, P., K. Sauer, D. G. Davies, and J. W. Costerton. 2002. Biofilms as complex differentiated communities. *Annu. Rev. Microbiol.* **56**: 187–209.
 27. SYBYL molecular modeling software; Tripos Inc., 1699. South Hanley Rd, Suite 303, St. Louis, MO 63144, U.S.A.
 28. The Center for Biofilm Engineering. 2003. Standardized Biofilm Methods Team For BioSurface Technologies, Inc. *CDC Biofilm Reactor Operator's Manual*, August.
 29. Zhang, R. G., T. Pappas, J. L. Brace, P. C. Miller, T. Oulmassov, J. M. Molyneaux, J. C. Anderson, J. K. Bashkin, S. C. Winans, and A. Joachimiak. 2002. Structure of a bacterial quorum-sensing transcription factor complexed with pheromone and DNA. *Nature* **417**: 971–974.